Preprints of the 20th World Congress
The International Federation of Automatic Control
Toulouse, France, July 9-14, 2017

Angular velocity and torque estimation from vector measurements

Lionel Magnis * **Nicolas Petit** **

* *Lycée Claude Bernard, 1 avenue du Parc des Princes, 75016 Paris, France*
** *MINES ParisTech, PSL Research University, CAS - Centre automatique et systèmes, 60 bd St Michel, 75272 Paris, France*

Abstract: We propose a technique for estimating the angular velocity of a rigid body and the torque applied to it, from vector measurements. Unlike the approaches reported in the literature, the method does not use attitude information or rate gyros as input data. Instead, vector measurements are directly filtered through a nonlinear observer. Convergence is proven. Simulation results illustrate the potential of the method for various aerospace applications, including estimation of reorientation torques for satellites, estimation of sublimation torques on an asteroid, estimation of eddy current damping torques on space debris.

Keywords: Inertial sensors; angular velocity; nonlinear observer; state observers; satellite control applications; torques estimation; linear damping estimation

1. INTRODUCTION

With the advances in low-cost sensors, several tasks of state estimation and, in particular, navigation, now appear to be feasible at a fraction of the cost of state-of-the-art high-end solutions. In these approaches, data fusion and filtering algorithms compensate for the imperfections of measurements provided by low-cost technologies. This is the case in many fields of engineering, including air vehicles, UAVs, guided munitions, sounding rockets and space applications, see e.g. Hua et al. (2014); Bekkeng and Psiaki (2008); Springmann and Cutler (2014); Lee et al. (2008); Shake et al. (2013); Springmann et al. (2012); Changey et al. (2012, 2014); Changey et al. (2013); Yu et al. (2016) amid numerous references.

Among state-estimation tasks, a central question is the reconstruction of the angular velocity as illustrated in numerous recent works, see e.g. Akella et al. (2015); Rafael et al. (2016); Wu and Lee (2015); Thienel and Sanner (2007); Berkane and Tayebi (2016); Magnis and Petit (2015). In the literature, several methods have been proposed to address this general question. One straightforward solution is to use a strap-down rate gyro (see Titterton and Weston (2004)) to directly measure angular velocity; however, since these are relatively fragile and expensive components, and are prone to drift, some other type of solution is often preferred. A *two-step approach* is commonly employed: the *first step* is to determine attitude from vector measurements (i.e., onboard measurement of reference vectors) within a fixed frame. Vector measurements play a fundamental role in the problem of attitude determination, as discussed in a recent survey (see Crassidis et al. (2007)). In a nutshell: when two independent vectors are measured by vector sensors attached to a rigid body, its attitude is simply defined as the solution of the classic Wahba's problem (see Wahba (1965)). This formulates a minimization problem in which the rotation matrix from a fixed frame to the body frame is the unknown. The *second step* is to reconstruct angular velocities from the attitude. At any instant, full attitude information can be obtained, as exposed in numerous references in various contexts such as Shuster (1978, 1990); Bar-Itzhack (1996); Choukroun (2003); Benziane et al. (2014); Tayebi et al. (2013); Grip et al. (2012a). Although angular velocity can be estimated from a time differentiation once the attitude is known, at least in principle, this process is disturbed by noise. To deal with this issue, introducing *a priori* information in the estimation process is a valuable technique for filtering noise from the estimates. For this reason, numerous observers using the Euler equations for a rigid body have been proposed to estimate angular velocity (or angular momentum, which is equivalent) from full attitude information (see Salcudean (1991); Thienel and Sanner (2007); Sunde (2005); Jorgensen and Gravdahl (2011)). Aside from this two-step approach, a more direct way of reconstructing the angular velocity can be considered. This employs an algorithm that uses vector measurements in a straightforward manner.

In two recent papers (Magnis and Petit (2017, 2016)) a nonlinear observer has been proposed. It reconstructs the angular velocity of a rotating rigid body from vector measurements *directly* by bypassing the relatively laborious first step of attitude estimation. The main limitation was that full knowledge of the torque applied to the rigid body was assumed. In the present work, we extend this new observer to allow a slowly varying torque to be estimated, opening broader possibilities for the above applications. Some examples are presented to illustrate the approach. We believe that the contributions presented here will be valuable to practitioners facing the problems under consideration and pave the way for future extensions and combinations. These extensions (and their proof of convergence) are not particularly difficult, but the equations,

which are directly implementable, will hopefully be useful for direct practical use. As is expected from such observers, the computational footprint is less compared to extended Kalman filters (EKF).

The paper is organized as follows. In Section 2, we introduce the notations and the problem statement. We analyze the attitude dynamics (rotation and Euler equations) and relate the analysis to measurements. In Section 3, we define a nonlinear observer with extended state and output injection and prove its convergence. Illustrative simulation results are given in Section 4. The scenarios under consideration include *impulsive torques* such as those generated by reaction control systems (RCS) for satellite attitude control, *sublimation torques* on an asteroid, and *eddy current damping torques* on space debris. In these scenarios, the assumption of piecewise constant or slowly varying torque is instrumental in the reconstruction. Conclusions are given in Section 5.

2. NOTATIONS AND PROBLEM STATEMENT

2.1 Notations

All frames considered in the following are orthonormal bases of $\mathbf{R}^3$. Vectors in $\mathbf{R}^3$ are written in lower-case x. $|x|$ is the Euclidean norm of x. $[x_\times]$ is the skew-symmetric cross-product matrix associated with x, i.e. $[x_\times]y = x \times y$, namely,

$$[x_\times] \triangleq \begin{pmatrix} 0 & -x_3 & x_2 \\ x_3 & 0 & -x_1 \\ -x_2 & x_1 & 0 \end{pmatrix}$$

where x_1, x_2, x_3 are the coordinates of x in the standard basis of $\mathbf{R}^3$. Vectors in higher dimension are written in upper-case X. $|X|$ designates the Euclidean norm of X. For any matrix $A \in \mathbf{R}^{n\times n}$, $\|A\|$ is the norm induced by the Euclidean norm in $\mathbf{R}^n$, namely,

$$\|A\| = \max_{X\in\mathbf{R}^n,\ |X|=1} |AX|.$$

For a vector valued function $f : \mathbf{R}^n \to \mathbf{R}^n$, ∇f is the Jacobian matrix of f. For real-valued functions $V(t, X)$ of time t and space X, ∇V is the gradient with respect to the space variable (i.e. $\nabla V = \frac{\partial V}{\partial X}$) and $\dot V$ is the derivative of $t \mapsto V(t, X(t))$ when $X(t)$ satisfies some differential equation.

2.2 Problem statement

Figure 1 shows the system being considered. Consider a rigid body rotating with respect to an inertial frame $\mathcal{R}_i$. Note R is the rotation matrix from $\mathcal{R}_i$ to a body frame $\mathcal{R}_b$ attached to the rigid body and ω is the corresponding angular velocity vector, expressed in $\mathcal{R}_b$. Assuming that the body rotates under the influence of an external torque τ (which is null in the case of free rotation), the variables R and ω are governed by the following differential equations:

$$\dot R = R[\omega_\times] \tag{1}$$

$$\dot\omega = J^{-1}\left(J\omega \times \omega + \tau\right) \tag{2}$$

where $J = \mathrm{diag}(J_1, J_2, J_3)$ is the inertia matrix [1]. This matrix is assumed to be known. In the literature, Eq. (2)

[1] Without restriction, we consider that the axes of $\mathcal{R}_b$ are aligned with the principal axes of inertia of the rigid body.

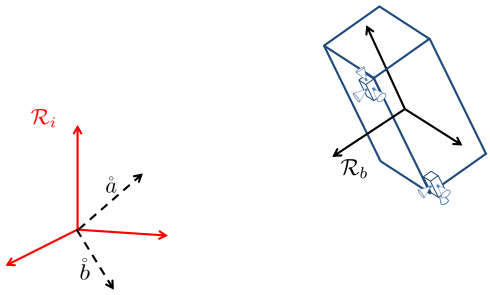

Fig. 1. Inertial frame, reference vectors, rigid body and body frame. Control torques can be generated by reaction thrusters, for example.

is referred to as the set of Euler equations for a rotating rigid body (see Landau and Lifchitz (1982)). The torque τ may result from control inputs or disturbances [2]. For clarity we note

$$E(\omega) \triangleq J^{-1}\left(J\omega \times \omega\right), \quad p \triangleq J^{-1}\tau$$

so that the Euler equations are simply written as

$$\dot\omega = E(\omega) + p.$$

We assume that there are two linearly independent reference unit vectors $\mathring{a}, \mathring{b}$ constant in $\mathcal{R}_i$, and that sensors arranged on the rigid body allow the measurement of the corresponding unit vectors expressed in $\mathcal{R}_b$. Namely, the measurements are

$$a(t) \triangleq R(t)^T\mathring{a}, \quad b(t) \triangleq R(t)^T\mathring{b} \tag{3}$$

which satisfy, by construction,

$$\dot a = a \times \omega, \quad \dot b = b \times \omega. \tag{4}$$

For implementation, the sensors might be, for example, Sun sensors, magnetometers or accelerometers, among others; the actual choices depend on the application under consideration. We now formulate some assumptions and a problem statement.

Assumption 1. τ is slowly varying [3] (so is p). It is not known but it generates a rotation such that ω is bounded: $|\omega(t)| \le \omega_{\max}$ at all times t.

Problem 1. Under Assumption 1, find estimates $(\hat\omega, \hat p)$ of (ω, p) from the vector measurements a, b defined in Eq. (3).

3. OBSERVER DESIGN AND ANALYSIS OF CONVERGENCE

3.1 Observer definition

When the torque p is known, a nonlinear observer of ω can be designed (see Magnis and Petit (2017)). Building

[2] In the case of a satellite, for instance, the torque could be generated by, among other possibilities, inertia wheels, magnetorquers or reaction thrusters as represented in Fig. 1.

[3] This assumption will be used to model these variables as constants, as is often done in linear observer design. Here "slow" means with respect to "fast" variables which are the other variables (directions), in the mathematical sense of singular perturbations of Kokotovic and Khalil (1986), e.g. . If needed, e. g. if these inputs signals are constantly and vastly changing, this assumption can be alleviated by considering that these variables are modeled as the response of a suitably chosen dynamical system or that only some high-order derivatives of these variables are constants, so that a finite number of state extension are required as exposed in the seminal work of Hostetter and Meditch (1973).

on this previous work, we here solve the general problem using the following extended observer

$$\left.\begin{aligned}\dot{\hat{a}} &= a\times\hat{\omega}+k(a-\hat{a})\\ \dot{\hat{b}} &= b\times\hat{\omega}+k(b-\hat{b})\\ \dot{\hat{\omega}} &= E(\hat{\omega})+\hat{p}+k^2\left(a\times\hat{a}+b\times\hat{b}\right)\\ \dot{\hat{\varpi}} &= E(\hat{\omega})+\gamma_1\sqrt{k}(\hat{\omega}-\hat{\varpi})+\hat{p}\\ \dot{\hat{p}} &= \gamma_2 k(\hat{\omega}-\hat{\varpi})\end{aligned}\right\} \tag{5}$$

where $k,\gamma_1,\gamma_2>0$ are constant tuning parameters. The inputs of this observer are the two vector measurements a and b; the outputs are $\hat{w}$ and $\hat{p}$, which are estimates of the angular velocity w and the applied torque p.

3.2 Error dynamics

To study the convergence of this observer, we introduce the scaled errors

$$\begin{aligned}X &= \begin{pmatrix} a-\hat{a}\\ b-\hat{b}\\ \dfrac{\omega-\hat{\omega}}{k}\end{pmatrix} \triangleq \begin{pmatrix}X_1\\X_2\\X_3\end{pmatrix}\in\mathbf{R}^9\\ Y &= \begin{pmatrix}\dfrac{\omega-\hat{\varpi}}{k}\\ \dfrac{p-\hat{p}}{k\sqrt{k}}\end{pmatrix} \triangleq \begin{pmatrix}Y_1\\Y_2\end{pmatrix}\in\mathbf{R}^6\end{aligned} \tag{6}$$

which are governed, with the assumption $\dot{p}=0$, using $\hat{\omega}-\hat{\varpi}=-kX_3+kY_1$, by

$$\left.\begin{aligned}\dot{X}_1 &= -kX_1+ka\times X_3\\ \dot{X}_2 &= -kX_2+kb\times X_3\\ \dot{X}_3 &= k\left(a\times X_1+b\times X_2\right)+\frac{E(\omega)-E(\hat{\omega})}{k}+\sqrt{k}Y_2\\ \dot{Y}_1 &= -\gamma_1\sqrt{k}Y_1+\sqrt{k}Y_2+\gamma_1\sqrt{k}X_3+\frac{E(\omega)-E(\hat{\omega})}{k}\\ \dot{Y}_2 &= -\gamma_2\sqrt{k}Y_1+\gamma_2\sqrt{k}X_3\end{aligned}\right\} \tag{7}$$

In the next section, we show that, for sufficiently large gain k, system (7) has local uniform exponential stability, thus providing a solution to Problem 1. Indeed, when X_3 and Y_2 go to 0, we have

$$\omega(t)-\hat{\omega}(t)\to 0,\quad p-\hat{p}(t)\to 0,\quad \text{as}\quad t\to+\infty.$$

Following (Khalil, 1996, Th. 3.13), we establish the exponential stability of the linearization about the origin $X=0$, $Y=0$ and conclude on the nonlinear dynamics. Linearization yields

$$\left.\begin{aligned}\dot{X} &= kA_1(t)X+\xi\\ \dot{Y} &= \sqrt{k}A_2Y+\zeta\end{aligned}\right\} \tag{8}$$

with

$$A_1(t)\triangleq\begin{pmatrix}-I & 0 & [a(t)_\times]\\ 0 & -I & [b(t)_\times]\\ [a(t)_\times] & [b(t)_\times] & 0\end{pmatrix}$$

$$\xi\triangleq\begin{pmatrix}0\\0\\ \nabla E(\omega)X_3+\sqrt{k}Y_2\end{pmatrix}$$

$$A_2\triangleq\begin{pmatrix}-\gamma_1 & 1\\ -\gamma_2 & 0\end{pmatrix},\quad \zeta\triangleq\begin{pmatrix}\gamma_1\sqrt{k}X_3+\nabla E(\omega)X_3\\ \gamma_2\sqrt{k}X_3\end{pmatrix}.$$

Thus, (8) appears as the interconnection of two systems

$$\dot{X}=kA_1(t)X \tag{9}$$

$$\dot{Y}=\sqrt{k}A_2Y \tag{10}$$

perturbed by the respective input term ξ,ζ, as pictured in Fig. 2.

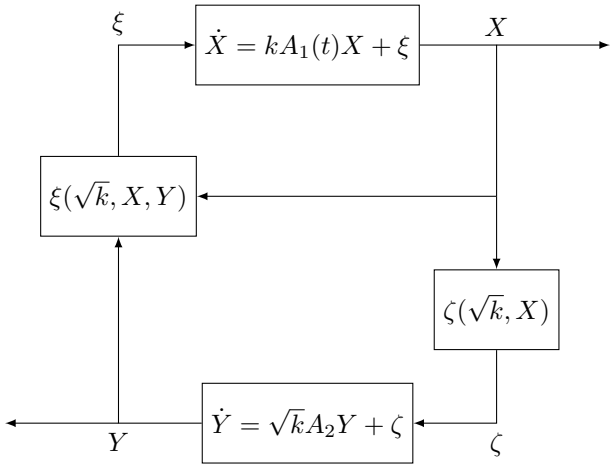

Fig. 2. Interconnection of systems (9)-(10)

3.3 Convergence proof

The proof is organized in distinct steps detailed below, resulting in the statement of Theorem 1.

Step 1: recall on the asymptotic behavior of the X-subsystem A detailed analysis of the time varying matrix $A_1(t)$ presented in Magnis and Petit (2017) shows the existence of a Lyapunov function $V_1(t,X)$ and constants

$$0<\alpha_1\leq\beta_1 \tag{11}$$

depending only on the (constant) value of the scalar product $\mathring{a}^T\mathring{b}$, such that for all (t,X)

$$\begin{aligned}&\alpha_1|X|^2\leq V_1(t,X)\leq\beta_1|X|^2\\ &|\nabla V_1(t,X)|\leq 2\beta_1|X|\\ &\dot{V}(t,X)=-k|X|^2\end{aligned}$$

where the total derivative is taken along the trajectories of system (9).

Step 2: study of the Y-system For any choice of $\gamma_1,\gamma_2>0$, A_2 has eigenvalues λ_1,λ_2 with strictly negative real parts $\Re(.)$. We assume that $\gamma_1^2\neq 4\gamma_2$ such that $\lambda_1\neq\lambda_2$. Note v_1,v_2 are two associated eigenvectors, $P=[v_1\ v_2]$ is the corresponding invertible matrix and $\lambda=-\max(\Re(\lambda_1),\Re(\lambda_2))$. We have, for all $Y\in\mathbf{R}^2$,

$$e^{\sqrt{k}A_2t}Y=P\begin{pmatrix}e^{\sqrt{k}\lambda_1 t} & 0\\ 0 & e^{\sqrt{k}\lambda_2 t}\end{pmatrix}P^{-1}Y$$

from which we deduce

$$|e^{\sqrt{k}A_2t}Y|\leq\|P\|\left\|P^{-1}\right\|e^{-\sqrt{k}\lambda t}|Y|$$

Defining V_2 as

$$\begin{aligned}V_2(Y)&\triangleq\sqrt{k}\ Y^T\int_0^\infty e^{\sqrt{k}A_2^Tt}e^{\sqrt{k}A_2t}dt\ Y\\ &=\sqrt{k}\int_0^\infty|e^{\sqrt{k}A_2^Tt}Y|^2dt\end{aligned}$$

we have, for all Y (see e.g. Khalil (1996)),

$$V_2(Y) \geq \frac{1}{2\left\|A_2\right\|}|Y|^2 \triangleq \alpha_2|Y|^2 \tag{12}$$

and also

$$V_2(Y) \leq \frac{\|P\|^2\left\|P^{-1}\right\|^2}{2\lambda} \triangleq \beta_2|Y|^2. \tag{13}$$

Finally, by upper bounding the gradient of the quadratic function V_2, we obtain

$$|\nabla V_2(Y)| \leq 2\beta_2|Y|.$$

Moreover, along the trajectories of (10),

$$\dot{V}_2(Y) = -\sqrt{k}|Y|^2.$$

Step 3: connecting the subsystems We now investigate the convergence of the interconnection. Consider the candidate Lyapunov function

$$V(t,(X,Y)) \triangleq V_1(t,X) + V_2(Y).$$

Note

$$\alpha \triangleq \min(\alpha_1,\alpha_2), \quad \beta \triangleq \max(\beta_1,\beta_2), \quad Z \triangleq \begin{pmatrix} X \\ Y \end{pmatrix}$$

We have

$$\alpha|Z|^2 \leq V(t,Z) \leq \beta|Z|^2$$

and the derivative of V along the trajectories of (7) satisfies

$$\dot{V}(t,Z) = -k|X|^2 + \nabla V_1(t,X)\xi - \sqrt{k}|Y|^2 + \nabla V_2(Y)\zeta.$$

As shown by direct calculation in Magnis and Petit (2017), we have

$$\|\nabla E(\omega)\| \leq \sqrt{2}\omega_{\max}.$$

Hence, the perturbation (coupling) terms are bounded by

$$\begin{aligned} |\xi| &\leq \sqrt{2}\omega_{\max}|X| + \sqrt{k}|Y| \\ |\zeta| &\leq \left(\sqrt{2}\omega_{\max} + (\gamma_1+\gamma_2)\sqrt{k}\right)|X|. \end{aligned}$$

It follows that

$$\begin{aligned} \dot{V}(t,Z) &\leq -k|X|^2 + 2\beta_1\sqrt{2}\omega_{\max}|X|^2 \\ &\quad + 2\sqrt{k}\beta_1|X||Y| - \sqrt{k}|Y|^2 \\ &\quad + 2\beta_2\left(\sqrt{2}\omega_{\max} + (\gamma_1+\gamma_2)\sqrt{k}\right)|X||Y| \end{aligned} \tag{14}$$

$$\begin{aligned} &= \sqrt{k}Z^T\begin{pmatrix} -\sqrt{k} & \beta_1+\beta_2(\gamma_1+\gamma_2) \\ \beta_1+\beta_2(\gamma_1+\gamma_2) & -1 \end{pmatrix}Z \\ &\quad + 2\beta_1\sqrt{2}\omega_{\max}|X|^2 + 2\beta_2\sqrt{2}\omega_{\max}|X||Y|. \end{aligned} \tag{15}$$

Interestingly, for sufficiently large k, the symmetric matrix

$$M \triangleq \begin{pmatrix} -\sqrt{k} & \beta_1+\beta_2(\gamma_1+\gamma_2) \\ \beta_1+\beta_2(\gamma_1+\gamma_2) & -1 \end{pmatrix}$$

is definite negative. Therefore, by choosing sufficiently large k, the first term in (15) is made dominant over the other terms that are not scaled by $\sqrt{k}$. Under these conditions, $\dot{V}$ is definite negative and system (7) is uniformly exponentially stable.

Theorem 1. (Solution to Problem 1). Consider Problem 1 where the unknown torque to be estimated is constant. For any choice of $\gamma_1,\gamma_2 > 0$, the observer (5) defines an error (6) which, for sufficiently large $k > 0$, converges locally uniformly exponentially to 0.

Remark 1. As α,β do not depend on k, the convergence is arbitrarily rapid when k grows to infinity. For practical applications, choosing large values for k increases the sensitivity to noise, so a natural recommendation is to consider only reasonable values for k. Implicitly, large value of k allow to converge over short horizons, over which the assumption of constant torque is numerically legit thanks to Assumption 1 of slow variations.

Remark 2. In (12), (13), α_2,β_2 depend only on the choice of γ_1,γ_2.

Remark 3. To account for more general torque models (e.g. piecewise affine time-varying signals, as considered below)

$$\dot{p} = p_1, \quad \dot{p}_1 = 0$$

the observer can be further extended in the form

$$\left.\begin{aligned} \dot{\hat{a}} &= a\times\hat{\omega} + k(a-\hat{a}) \\ \dot{\hat{b}} &= b\times\hat{\omega} + k(b-\hat{b}) \\ \dot{\hat{\omega}} &= E(\hat{\omega}) + \hat{p} + k^2\left(a\times\hat{a} + b\times\hat{b}\right) \\ \dot{\hat{\varpi}} &= E(\hat{\omega}) + \gamma_1\sqrt{k}(\hat{\omega}-\hat{\varpi}) + \hat{p} \\ \dot{\hat{p}} &= \hat{p}_1 + \gamma_2 k(\hat{\omega}-\hat{\varpi}) \\ \dot{\hat{p}}_1 &= \gamma_3 k^{\frac{3}{2}}(\hat{\omega}-\hat{\varpi}) \end{aligned}\right\} \tag{16}$$

with $k,\gamma_1,\gamma_2,\gamma_3 > 0$. The convergence analysis is identical. The generalization to signals having a zero n-th order derivative $\dot{p} = p_1, \quad \dot{p}_1 = p_2, \quad \ldots, \quad \dot{p}_n = 0$ is straightforward.

4. SIMULATION RESULTS AND APPLICATIONS

In this section, we consider several illustrative examples. For the sake of accuracy of implementation, the reference dynamics (2)-(4) and state observer (5) are simulated using the Runge-Kutta 4 method. This is an important point, as the integration of Euler equations $E(.)$ requires a good level of accuracy to avoid numerical divergence. The sampling (measurement) period is specified in each example.

4.1 Estimating torques during a reorientation maneuver (Heaviside step torques)

The first problem we consider is the estimation of torques during a satellite reorientation maneuver. We consider a satellite which is a parallelepiped of size 90 × 130 × 170 [cm^3] and mass 150 [kg] homogeneously distributed. The general behavior of the observer is represented in Fig. 3. In this simulation, the torques are Heaviside step inputs. Such signals are employed in optimal reorientation maneuvers (as described in Shen and Tsiotras (1999); Bai and Junkins (2009)). The sampling time is 0.1 s. The proposed observer produces converging estimates for the (vector) angular velocity and for the torques. Each step variation of the torque induces a transient error for $\hat{\tau}$ and $\hat{\omega}$. Even then, the angular velocity error does not exceed 5 [°/s] for a nominal value of ω of about 250 [°/s]. The role of the tuning gain k is seen in Fig. 4, which shows the observer performance for increasing values of k and fixed values $\gamma_1 = 1, \gamma_2 = 0.2$. As expected, the convergence is better for larger values of the gain. Thus, the tuning of k will result from a trade-off between performance and noise reduction. Finally, Fig. 5 stresses the role of the discussed observer extension. Torque signals that are not piecewise constant but slowly varying are estimated well using the extension, by reducing asymptotic bias.

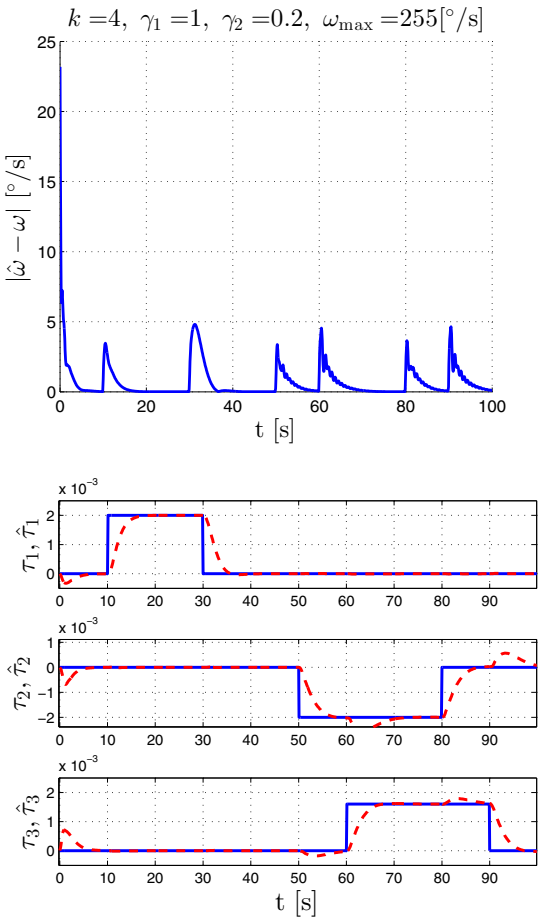

Fig. 3. Convergence of the observer. Top: angular velocity error. Bottom: torque (solid line) and estimated torque (dashed line).

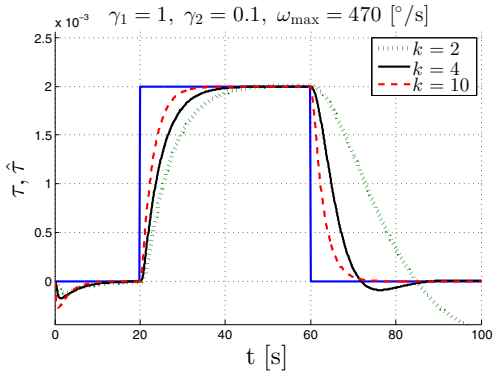

Fig. 4. Convergence of estimated torque improves with increasing k.

4.2 Estimating sublimation torques (impulsive and noisy torques)

In this second example, we wish to estimate a torque signal with no particular signature except that it is non-zero for short periods only. This property is representative of torques produced by sublimation on asteroids, that is, the sudden transformation into water vapor of ice on the surface of an asteroid upon exposure to sunlight.

Very generally, the monitoring of rotation states of asteroids and comets has been the subject of numerous studies.

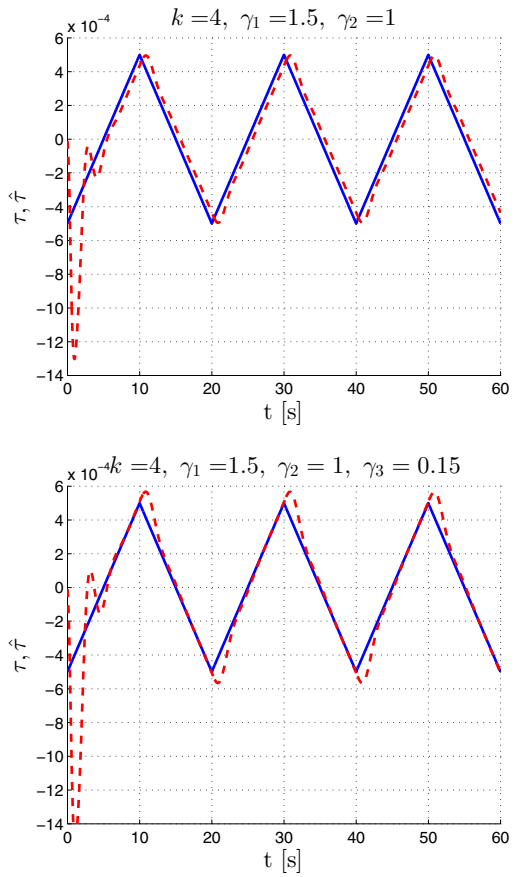

Fig. 5. Top: Observer (5) tracks slowly varying torques with phase shift. Bottom: Extended observer (16) reduces the residual error.

This subject is of importance as the spin of an asteroid can affect its orbit in quite a subtle way due to the Yarkovsky effect (see Rubincam (2000)), causing uncertainty in the prediction of future trajectories. Usually, the time-series analysis of emitted light, or "light curves" (see Lorenz (2006)), is employed to determine the spin. The frequent cases of pure long-axis mode (LAM) rotation is a (to some extent) resolved problem; however, numerous recent studies have reported that several comets and asteroids have more complex rotations (e.g., 1P/Halley, and (4179) Toutatis –see Mueller et al. (2002); Samarasinha and Belton (1995)). In such cases, the light curves are difficult to analyze. Following the ideas developed in this article, a suggested alternative technique is as follows: assuming that a set of suitable sensors could be attached to the object (as achieved by the Rosetta lander –see Ulamec et al. (2015)) and that their measurements could be processed, at least for some time interval, it would be possible to reconstruct the torques produced by cometary activity, in particular the sublimation-induced torques, using the approach proposed here.

Figure 6 shows the estimated torque for a simulated Halley-like comet considered here as an ellipsoid with semi-axes $16 \times 8 \times 7.999$ km^3 and mass 2.10^{14} kg homogeneously distributed, and an initial rotation period of 12 hours. The magnitude of the torque was chosen in accordance with the calculations described in Samarasinha and Belton (1995). For realism, some measurement noise was added, which explains the shape of the dashed curve.

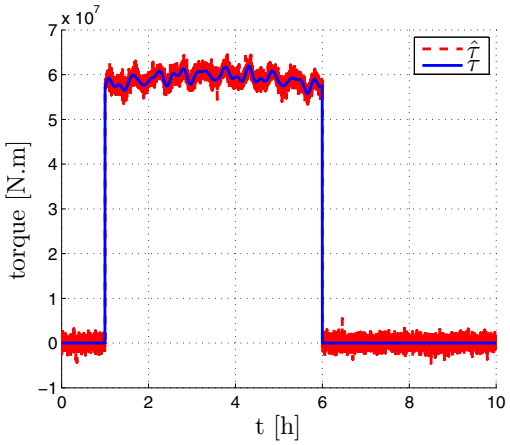

Fig. 6. Estimation of sublimation torques for a Halley-like comet.

4.3 Estimating eddy-current braking, i.e. induced linear damping torques

This third example considers a slowly varying torque, proportional to the angular velocity. This is representative of torques produced by magnetic braking inside space debris.

Space debris orbiting in the magnetosphere are subject to magnetic braking stemming from eddy currents created in their spinning bodies. As developed in Praly et al. (2011, 2012), the torques driving the spin motion of an empty, thin-walled body (e.g., the H10 stage of the Ariane 4 rocket), are of the form

$$\tau \approx \begin{pmatrix} c_1 & 0 & 0 \\ 0 & c_2 & 0 \\ 0 & 0 & c_3 \end{pmatrix} w$$

where c_1, c_2, c_3 are positive parameters proportional to the magnitude of the local magnetic field. These parameters also depend on the rotational axis of the long-term rotation of the object (axial spin or flat spin). Along typical orbits, the torques defined above yield a quasi-linear asymptotic decay, with decay times ranging from 20 days (axial spin) to 250 days (flat spin). In Praly et al. (2011), a finite element method simulation was conducted to estimate the induction phenomenon, in which the model of the spinning object was simplified to a symmetrical cylinder with semi-spherical ends. Certainly, some error was generated by this approximation, and it would be interesting to use experimental data to improve the model. The observer proposed in this article can be used for such an objective. The error we take into consideration appears in the torque-generation law, where we assume that the torque is actually linearly dependent on the angular velocity through an unknown matrix T

$$\tau = Tw$$

We can modify the above observer to estimate the whole matrix T, or equivalently $P \triangleq J^{-1}T$. To address this problem, a *further extension* of the proposed observer is needed, with the idea of interconnecting the X system (9) with another exponentially stable system. In detail, while the Euler equations become

$$\dot{\omega} = E(\omega) + P\omega$$

we propose the following observer

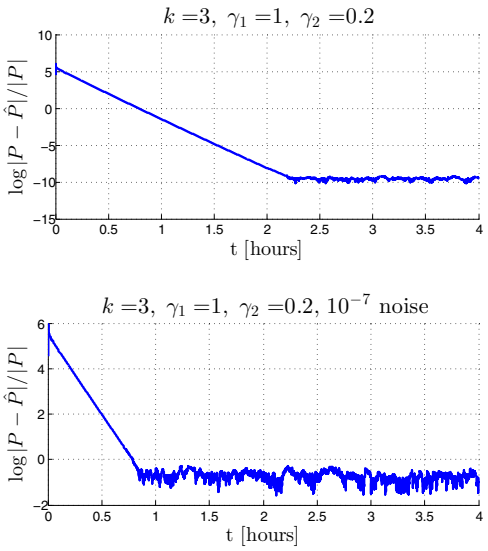

Fig. 7. Estimation of P without noise (top) and with 10^{-7} noise level (bottom). ($\log_{10}$ scale).

$$\left.\begin{aligned} \dot{\hat{a}} &= a \times \hat{\omega} + k(a - \hat{a}) \\ \dot{\hat{b}} &= b \times \hat{\omega} + k(b - \hat{b}) \\ \dot{\hat{\omega}} &= E(\hat{\omega}) + \hat{P}\hat{\omega} + k^2\left(a \times \hat{a} + b \times \hat{b}\right) \\ \dot{\hat{\varpi}} &= E(\hat{\omega}) + \hat{P}\hat{\omega} + \gamma_1(\hat{\omega} - \hat{\varpi}) \\ \dot{\hat{P}} &= \gamma_2(\hat{\omega} - \hat{\varpi})\hat{\omega}^T \end{aligned}\right\} \quad (17)$$

with $k, \gamma_1, \gamma_2 > 0$. Consider the observer error

$$X \triangleq \begin{pmatrix} a - \hat{a} \\ b - \hat{b} \\ \dfrac{\omega - \hat{\omega}}{k} \end{pmatrix} \triangleq \begin{pmatrix} X_1 \\ X_2 \\ X_3 \end{pmatrix} \in \mathbf{R}^9,$$

$$Y \triangleq \frac{1}{k}\begin{pmatrix} \omega - \hat{\varpi} \\ P - \hat{P} \end{pmatrix} \triangleq \begin{pmatrix} Y_1 \\ Y_2 \end{pmatrix} \in \mathbf{R}^3 \times \mathbf{R}^{3\times 3}.$$

Note that Y_2 is a 3×3 matrix. The linearized error system around $X = 0, Y = 0$ is

$$\dot{X} = kA(t)X + \begin{pmatrix} 0 \\ 0 \\ \nabla E(\omega)X_3 + PX_3 + Y_2\omega \end{pmatrix}$$

$$\dot{Y}_1 = -\gamma_1 Y_1 + Y_2\omega + \nabla E(\omega)X_3 + PX_3 + \gamma_1 X_3$$

$$\dot{Y}_2 = -\gamma_2 Y_1\omega^T + \gamma_2 X_3\omega^T.$$

In this form, the error system appears as an interconnection of the exponentially stable system (9) with the Y system

$$\dot{Y}_1 = -\gamma_1 Y_1 + Y_2\omega, \quad \dot{Y}_2 = -\gamma_2 Y_2\omega^T. \quad (18)$$

The convergence analysis is similar: establish the exponential stability of the Y system, and derive conditions such that the interconnection maintains stability. Briefly, a candidate Lyapunov function for system (18) would be

$$V(Y) = \frac{\gamma_2}{2}|Y_1|^2 + \frac{\gamma_1}{2}\mathrm{Tr}\left(Y_2^T Y_2\right)$$

(where Tr (.) is the trace operator) which is positive definite and satisfies $\dot{V}(Y) = -\gamma_1\gamma_2|Y_1|^2$ along the trajectories of (18). Uniform exponential stability requires a persistent excitation-like assumption on ω guaranteeing that $\omega(t)$ persistently reaches all the directions in $\mathbf{R}^3$.

This modified observer was tested in a simulation with sampling time 0.2 s, the following inertia and damping

matrices

$$J = \begin{pmatrix} 1442 & 19 & 31 \\ 19 & 10799 & 113 \\ 31 & 113 & 10755 \end{pmatrix} \text{ [kg.m}^2\text{]}$$

$$P = 10^{-8} \begin{pmatrix} -39.7 & 0.06 & 0.1 \\ 0.07 & -4.5 & 0.05 \\ 0.1 & 0.05 & -4.5 \end{pmatrix} \text{ [s}^{-1}\text{]}$$

and $|\omega(0)| \simeq 60$ [°/s]. The results of the estimation of P are represented in Figure 7. In the absence of measurement noise, the relative error for P decreases from 10^6 to 10^{-10} within a few hours. With a noise level of 10^{-7}, the relative error reaches the asymptotic value of 10^{-1}, meaning that the coefficient of the P matrix (or T) is reconstructed with a 10% error.

Remark 4. Since the exponential stability comes from a persistent excitation assumption, arbitrarily fast convergence of the error system cannot be guaranteed when k increases to infinity.

5. CONCLUSIONS

In this article we have proposed a method of directly estimating the angular velocity and torques applied to a rigid body, from vector measurements. The method takes the form of a simple, nonlinear observer that produces real-time estimates of these variables. It represents a possible alternative to a gyroscope.

The computational footprint of the proposed observer is very limited compared to state-of-the-art alternatives such as EKF. This is an appealing feature if one wishes to employ low-power embedded systems with very limited computation capabilities. In other cases, we would recommend to compare the obtained results with an EKF. In this context, what the contributions of this article provide is a formal proof that the systems proposed for the various task of state reconstruction are indeed observable, in the sense that an observer with guaranteed convergence has been given. This is a handy result before any EKF can be implemented and tested.

Further extensions are possible. This observer can be adapted to various situations where uncertainties come into play, such as unknown coefficients in the governing equations, or randomness of torque signals. A subject directly connected to the presented results is the estimation of gyros biases and drift, which is a subject of great importance when gyros are present as explained in numerous contributions Choukroun et al. (2011); Metni et al. (2006); Bergamini et al. (2014); Grip et al. (2012b); Hamel and Mahony (2006); Mahony et al. (2008); Martin and Sarras (2016); Batista et al. (2011); Fourati and Belkhiat (2016) among others.

REFERENCES

Akella, M.R., Thakur, D., and Mazenc, F. (2015). Partial Lyapunov strictification: Smooth angular velocity observers for attitude tracking control. *Journal of Guidance, Control, and Dynamics*, 38(3), 442–451.

Bai, X. and Junkins, J.L. (2009). New results for time-optimal three-axis reorientation of a rigid spacecraft. *Journal of Guidance, Control, and Dynamics*, 32(4), 1071–1076.

Bar-Itzhack, I.Y. (1996). REQUEST - a new recursive algorithm for attitude determination. *Proceedings of the National Technical Meeting of The Institute of Navigation*, 699–706.

Batista, P., Silvestre, C., and Oliveira, P. (2011). Partial attitude and rate gyro bias estimation: observability analysis, filter design, and performance evaluation. *International Journal of Control*, 84(5), 895–903.

Bekkeng, J.K. and Psiaki, M. (2008). Attitude estimation for sounding rockets using microelectromechanical system gyros. *Journal of Guidance, Control, and Dynamics*, 31(3), 533–542.

Benziane, L., Benallegue, A., and Tayebi, A. (2014). Attitude stabilization without angular velocity measurements. In *2014 IEEE International Conference on Robotics and Automation (ICRA)*, 3116–3121.

Bergamini, E., Ligorio, G., Summa, A., Vannozzi, G., Cappozzo, A., and Sabatini, A.M. (2014). Estimating orientation using magnetic and inertial sensors and different sensor fusion approaches: Accuracy assessment in manual and locomotion tasks. *Sensors*, 14(10).

Berkane, S. Abdessameud, A. and Tayebi, A. (2016). Global exponential angular velocity observer for rigid body systems. In *Proc. of the 55th IEEE Conference on Decision and Control*.

Changey, S., Pecheur, E., Bernard, L., Sommer, E., Wey, P., and Berner, C. (2012). Real time estimation of projectile roll angle using magnetometers: In-flight experimental validation. In *Position Location and Navigation Symposium (PLANS), 2012 IEEE/ION*, 371–376.

Changey, S., Pecheur, E., and Brunner, T. (2014). Attitude estimation of a projectile using magnetometers and accelerometers, experimental validation. In *Position, Location and Navigation Symposium - PLANS 2014, 2014 IEEE/ION*, 1168–1173.

Changey, S., Pecheur, E., Wey, P., and Sommer, E. (2013). Real-time estimation of projectile roll angle using magnetometers: in-lab experimental validation. *EUCASS Proceedings Series*, 6, 35–44.

Choukroun, D. (2003). *Novel methods for attitude determination using vector observations.* Ph.D. thesis, Technion.

Choukroun, D., Cooper, L., and Berman, N. (2011). Spacecraft attitude estimation and gyro calibration via stochastic h_∞ filtering. In F. Holzapfel and S. Theil (eds.), *Advances in Aerospace Guidance, Navigation and Control: Selected Papers of the 1st CEAS Specialist Conference on Guidance, Navigation and Control*, 397–415. Springer Berlin Heidelberg, Berlin, Heidelberg.

Crassidis, J.L., Markley, F.L., and Cheng, Y. (2007). Survey of nonlinear attitude estimation methods. *Journal of Guidance, Control, and Dynamics*, 30(1), 12–28.

Fourati, H. and Belkhiat, D.E.C. (2016). *Multisensor Attitude Estimation: Fundamental Concepts and Applications.* CRC Press.

Grip, H.F., Fossen, T.I., Johansen, T.A., and Saberi, A. (2012a). Attitude estimation using biased gyro and vector measurements with time-varying reference vectors. *IEEE Transactions on Automatic Control*, 57(5), 1332–1338.

Grip, H.F., Fossero, T.I., Johansen, T.A., and Saberi, A. (2012b). A nonlinear observer for integration of GNSS and IMU measurements with gyro bias estimation. In

2012 American Control Conference (ACC), 4607–4612. IEEE.

Hamel, T. and Mahony, R. (2006). Attitude estimation on SO[3] based on direct inertial measurements. In *Proceedings 2006 IEEE International Conference on Robotics and Automation, 2006. ICRA 2006.*, 2170–2175. doi: 10.1109/ROBOT.2006.1642025.

Hostetter, G. and Meditch, J. (1973). Observing systems with unmmeasurable inputs. *IEEE Transactions on Automatic Control*, 18(3), 307–308.

Hua, M.D., Ducard, G., Hamel, T., Mahony, R., and Rudin, K. (2014). Implementation of a nonlinear attitude estimator for aerial robotic vehicles. *IEEE Transactions on Control Systems Technology*, 22(1), 201–213.

Jorgensen, U. and Gravdahl, J.T. (2011). Observer based sliding mode attitude control: Theoretical and experimental results. *Modeling, Identification and Control*, 32(3), 113–121.

Khalil, H.K. (1996). *Nonlinear Systems*. Prentice-Hall, second edition.

Kokotovic, P.V. and Khalil, H.K. (1986). *Singular Perturbations in Systems and Control*. IEEE Press, New York.

Landau, L. and Lifchitz, E. (1982). *Mechanics*. MIR Moscou, fourth edition.

Lee, H., Choi, Y.H., Bang, H.C., and Park, J.O. (2008). Kalman filtering for spacecraft attitude estimation by low-cost sensors. *KSAS International Journal*, 9(1), 147–161.

Lorenz, R.D. (2006). *Spinning Flight*. Springer.

Magnis, L. and Petit, N. (2016). Angular velocity nonlinear observer from single vector measurements. *Automatic Control, IEEE Transactions on*, 61(9), 2473–2483.

Magnis, L. and Petit, N. (2017). Angular velocity nonlinear observer from vector measurements. *Automatica*, 75, 46–53.

Magnis, L. and Petit, N. (2015). Gyroless Ball: estimation of angular velocity without gyroscope. Research report, MINES ParisTech. URL `https://hal-mines-paristech.archives-ouvertes.fr/hal-01239374`.

Mahony, R., Hamel, T., and Pflimlin, J.M. (2008). Nonlinear complementary filters on the special orthogonal group. *IEEE Transactions on Automatic Control*, 53(5), 1203–1218.

Martin, P. and Sarras, I. (2016). A simple global observer for attitude and gyro biases, arxiv:1604.03714. Technical report, MINES ParisTech.

Metni, N., Pflimlin, J.M., Hamel, T., and Souères, P. (2006). Attitude and gyro bias estimation for a VTOL UAV. *Control Engineering Practice*, 14(12), 1511 – 1520.

Mueller, B.E., Samarasinha, N.H., and Belton, M.J. (2002). The diagnosis of complex rotation in the lightcurve of 4179 Toutatis and potential applications to other asteroids and bare cometary nuclei. *Icarus*, 158(2), 305–311.

Praly, N., Hillion, M., Bonnal, C., Laurent-Varin, J., and Petit, N. (2012). Study on the eddy current damping of the spin dynamics of space debris from the ariane launcher upper stages. *Acta Astronautica*, 76, 145–153.

Praly, N., Petit, N., Bonnal, C., and Laurent-Varin, J. (2011). Study of the eddy current damping of the spin dynamics of spatial debris from the Ariane launcher. *Proceedings of the 4^{th} European Conference for Aerospace Sciences*.

Rafael, C.M., Saúl, S.G., Yu, T., and Haibo, J. (2016). Contraction based angular velocity observer for small satellites. In *2016 IEEE Aerospace Conference*, 1–10.

Rubincam, D.P. (2000). Radiative Spin-up and Spin-down of Small Asteroids. *Icarus*, 148, 2–11.

Salcudean, S. (1991). A globally convergent angular velocity observer for rigid body motion. *IEEE Transactions on Automatic Control*, 36(12), 1493–1497.

Samarasinha, N.H. and Belton, M.J. (1995). Long-term evolution of rotational states and nongravitational effects for Halley-like cometary nuclei. *Icarus*, 116(2), 340–358.

Shake, C.M., Saulnier, K., and Bevilacqua, R. (2013). Spacecraft attitude determination system using nano-optical devices and linux software libraries. *Journal of Aerospace Information Systems*, 10, 369–384.

Shen, H. and Tsiotras, P. (1999). Time-optimal control of axi-symmetric rigid spacecraft using two controls. *J. Guidance, Control and Dynamics*, 22(5), 682–694.

Shuster, M.D. (1978). Approximate algorithms for fast optimal attitude computation. *Proceedings of the AIAA Guidance and Control Conference*, 88–95.

Shuster, M.D. (1990). Kalman filtering of spacecraft attitude and the QUEST model. *The Journal of the Astronautical Sciences*, 38(3), 377–393.

Springmann, J.C. and Cutler, J.W. (2014). Flight results of a low-cost attitude determination system. *Acta Astronautica*, 99, 201–214.

Springmann, J.C., Sloboda, A.J., Klesh, A.T., Bennett, M.W., and Cutler, J.W. (2012). The attitude determination system of the rax satellite. *Acta Astronautica*, 75, 120–135.

Sunde, B.O. (2005). *Sensor Modelling and attitude determination for micro-satellites*. Master's thesis, NTNU.

Tayebi, A., Roberts, A., and Benallegue, A. (2013). Inertial vector measurements based velocity-free attitude stabilization. *IEEE Transactions on Automatic Control*, 58(11), 2893–2898.

Thienel, J.K. and Sanner, R.M. (2007). Hubble Space Telescope angular velocity estimation during the robotic servicing mission. *Journal of Guidance, Control, and Dynamics*, 30(1), 29–34.

Titterton, D. and Weston, J. (2004). *Strapdown Inertial Navigation Technology*. The American Institute of Aeronautics and Aeronautics, Reston, USA, 2 edition.

Ulamec, S., Biele, J., Blazquez, A., Cozzoni, B., Delmas, C., Fantinati, C., Gaudon, P., Geurts, K., Jurado, E., Küchemann, O., Lommatsch, V., Maibaum, M., Sierks, H., and Witte, L. (2015). Rosetta lander - philae: Landing preparations. *Acta Astronautica*, 107, 79 – 86.

Wahba, G. (1965). Problem 65-1: a least squares estimate of spacecraft attitude. *SIAM Review*, 7(3), 409.

Wu, T.H. and Lee, T. (2015). Angular velocity observer for velocity-free attitude tracking control on so(3). In *Control Conference (ECC), 2015 European*, 1824–1829.

Yu, J., Bu, X., Xiang, C., and Yang, B. (2016). Spinning projectile's attitude measurement using intersection ratio of magnetic sensors. *Proceedings of the Institution of Mechanical Engineers, Part G: Journal of Aerospace Engineering*.